Last millennium sedimentation in the Gulf of Cariaco (NE Venezuela): Evidence for morphological changes of gulf entrance and possible relations with large earthquakes

Iliana Aguilar, Christian Beck, Franck Audemard, Anne-Lise Develle, Mohammed Boussafir, Corina Campos, Christian Crouzet

C. R. Geoscience 348 (2016) 70–79

Contents lists available at ScienceDirect

Comptes Rendus Geoscience

www.sciencedirect.com

Stratigraphy, Sedimentology (Palaeoenvironment)

Last millennium sedimentation in the Gulf of Cariaco (NE Venezuela): Evidence for morphological changes of gulf entrance and possible relations with large earthquakes

Iliana Aguilar [a,b], Christian Beck [a,*], Franck Audemard [b], Anne-Lise Develle [c], Mohammed Boussafir [d], Corina Campos [e], Christian Crouzet [a]

[a] CNRS ISTerre, université Savoie–Mont-Blanc, 73376 Le Bourget-du-Lac, France
[b] Venezuelan Foundation for Seismological Research/FUNVISIS, El Llanito, Caracas, Venezuela
[c] CNRS EDYTEM, université Savoie-Mont-Blanc, 73376 Le Bourget-du-Lac, France
[d] Institut des Sciences de la Terre d'Orléans (ISTO), UMR 7327, CNRS/INSU, université d'Orléans, BRGM, 45071 Orléans, France
[e] Dpto. Ciencias de la Tierra, Sartenejas, Universidad Simón Bolívar, Caracas, Venezuela

ARTICLE INFO

Article history:
Received 5 July 2015
Accepted after revision 7 October 2015
Available online 30 November 2015

Handled by Isabelle Manighetti

Keywords:
El Pilar fault
Cariaco
Sedimentation
Geochemistry
Submarine landslides
Large earthquakes
Submarine paleoseismology

ABSTRACT

The Cariaco Basin and the Gulf of Cariaco in Venezuela are two major basins along the seismogenic El Pilar right lateral fault, among which the Cariaco Basin is a pull-apart. Both basins are sites of anoxia and organic-rich deposits. To examine whether the sediments in the Gulf of Cariaco have recorded traces of historical or prehistorical earthquakes, we extracted and analyzed twelve 1 m-long gravity cores, sampling the last millennium sedimentation. We focused on analyzing the sediment sources with different techniques (particle size analysis, XRF, loss on ignition tests, magnetic properties, Rock-Eval pyrolysis, ^{14}C dating). The results confirm that major upwelling occurs at the western gulf entrance and makes deep water flowing from the Cariaco Basin into the Gulf of Cariaco. These flows carry an organic-rich suspended load. Furthermore, we found evidence of a particular, widespread fine-grained siliciclastic deposit (named SiCL3) within the gulf, whose age suggests that it likely formed during the large 1853 AD earthquake that stroke the Cumaná city. We suggest that the earthquake-induced large submarine landslides that modified the topography of the gulf's entrance, which in turn promoted upwelling and open marine water flows from the Cariaco Basin. The layer SiCL3 would be the sediment load remobilized during this chain of events.

Introduction

The relative displacement between the South America and the Caribbean plates is mainly accommodated along the right lateral strike slip San Sebastian-El Pilar fault system, at the northern boundary of Venezuela (Fig. 1; Audemard et al., 2000, 2005; DeMets et al., 2000; Pérez et al., 2001; Stéphan et al., 1990; Symithe et al., 2015; Weber et al., 2001). In the eastern part of the fault system, named El Pilar fault or EPF, the plate boundary fault is underlined by a 1400 m-deep, 160 km-long, 50 km-wide, pull-apart basin, the Cariaco Basin (also named Cariaco Trough) (Schubert, 1979, 1982). Further east, the Gulf of Cariaco is a smaller (65 km-long, 15 km-wide) and shallower (85 m-deep) basin, connected to the Cariaco Basin. The former developed directly upon and along the EPF, on the northern side. The EPF fault accommodates most of the relative plate motions through a combination

* Corresponding author.
E-mail address: beck.christian7@gmail.com (C. Beck).

http://dx.doi.org/10.1016/j.crte.2015.10.001
1631-0713/

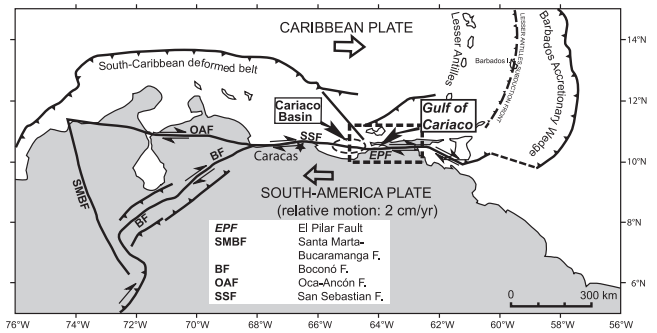

Fig. 1. Tectonic setting of the Gulf of Cariaco. Active faults from Audemard et al. (2000, 2005), DeMets et al. (2000), Pérez et al. (2001), Weber et al. (2001), Symithe et al. (2015).

of creep (~60%) and co-seismic offsets (~40%) (Audemard, 2007; Jouanne et al., 2011; Reinoza et al., 2015). The EPF fault has in particular produced large earthquakes (i.e. with estimated MSK intensities of IX/X; Audemard, 2007) over the last centuries; most have seriously affected the city of Cumaná (location in Fig. 2). In an attempt to estimate the seismogenic potential of the EPF fault, many studies have been conducted in the last decades, most were led by the Venezuelan Foundation for Seismological Investigations. Since the main section of the EPF fault (named "VE-13b" by Audemard, 2007) is offshore (Fig. 2), multiple high-resolution seismic reflection data have been acquired to analyze the fault and to search for information on its historical and prehistorical ruptures (Audemard et al., 2007; Van Daele et al., 2011). Subaqueous paleoseismology has also been conducted, using approaches previously developed along other seismogenic faults in Venezuela (Carrillo et al., 2008). These studies analyze the sedimentary content in short "gravity cores" (~1 m long) so as to search and identify sedimentary changes that might have resulted from large earthquake motions, as it was observed right after the most recent large earthquake in the area (M_w 6.9 Cariaco earthquake, Lorenzoni et al., 2012; Thunell et al., 1999).

The present paper focuses on this question, and explores the possible sedimentary signature of large historical earthquakes in the Gulf of Cariaco and in the eastern part of the Cariaco Basin. The eastern region of the Cariaco basin is interesting because it marks the entrance to the Gulf of Cariaco, and it is the site of a steep, 400 m-high, ~north–south-trending escarpment at the western edge of the Manzanares River delta (MRd in Fig. 2). The MRd delta is where the Cumaná city has developed. This delta is crosscut by the EPF fault. Therefore, we might expect that large historical and prehistorical earthquakes on the EPF fault in the area of Cumaná have disturbed the nearby eastern part of the Cariaco Basin, with possible consequences on the sedimentation within the Gulf of Cariaco.

To examine these hypotheses, we analyze the sedimentary content of 12 cores extracted in the Gulf of Cariaco. We focus on determining the sediment sources (based on mineralogy and geochemistry) and their distribution pattern. Previous results have suggested that upwelling at the basin–gulf junction significantly controlled the sediment sources (Gade, 1961; Okuda, 1981, 1982; Okuda et al., 1974, 1978). In turn, part of the upwelling might have been enhanced by historical large

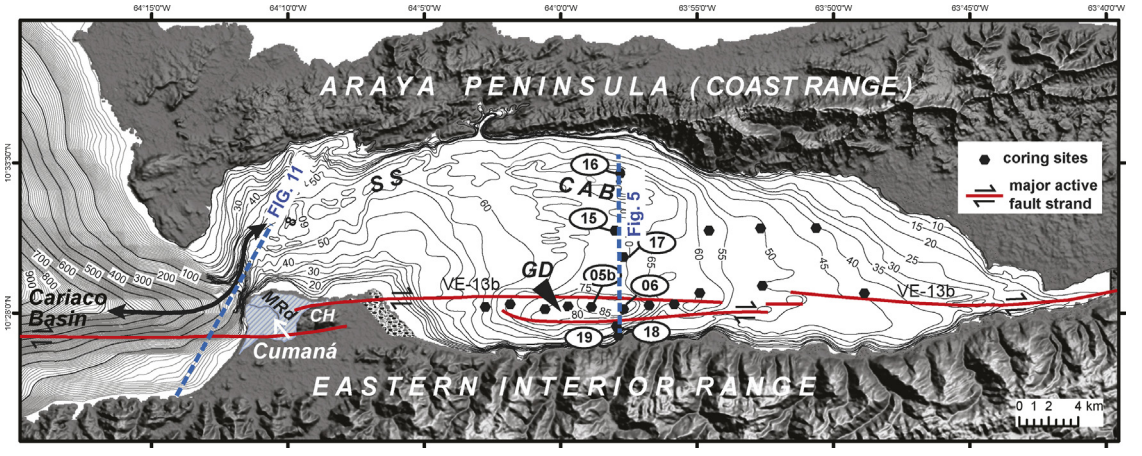

Fig. 2. (Color online). Geomorphic setting of the Gulf of Cariaco and of its connection with the Cariaco Basin. SS: Salazar Sill; CAB: Cerro Abajo Basin; GD: Guaracayal Deep; MRd: Manzanares River delta; CH: Caiguïre Hills. Bathymetry simplified from Caraballo (1982a). Shaded-relief map from Garrity et al. (2004).

earthquake disruptions of the basin–gulf junction morphology and topography.

1. Geological setting and sedimentary environment of the Gulf of Cariaco

1.1. Tectonic setting and characteristics of the Gulf of Cariaco catchment area

The offshore trace of the EPF in the Gulf of Cariaco has been identified in high-resolution seismic data (Audemard et al., 2007; Van Daele et al., 2011; Fig. 2). The fault trace appears segmented, with two large relay zones between its longest segments: the Garacayal pull-apart or "Garacayal deep" (GD, Fig. 2), and the Caiguïre Hills push-up (CH, Fig. 2). The entrance of the gulf is the site of the large Manzanares River delta.

According to historical archives (in Altez Ortega et al., 2004; Audemard, 2007; Grases, 1990), four major earthquakes with associated tsunami hit the City of Cumaná in 1530, 1853, 1929 and 1997. Reports indicate that 4–6 m- and 6 m-high run-up hit the Cumaná coast during the 1853 and 1929 events, respectively. Traces of Holocene paleo-tsunamis have also been found in coastal lagoons in the Manzanares River delta (Leal et al., 2014). Right after the M_w 6.9 1997 Cariaco earthquake, significant and long-lasting sediment resuspensions were observed in the eastern Cariaco Basin, and were attributed to earthquake-induced submarine landslides, most probably on the western slope of the Manzanares River delta (Lorenzoni et al., 2012; Thunell et al., 1999). Furthermore, inhabitants from both northeastern and southeastern coastal areas reported a lowering of the sea surface by several meters, but no subsequent inland overflowing. These observations suggest that a tsunami resulted from the 1997 earthquake, which induced east–west moving waves. The tsunami may have enhanced the observed sediment resuspensions.

The reliefs that bound the gulf's catchment area (Supplementary Material S1) are ~400 m a.s.l. in the Araya Peninsula and ~800 m a.s.l. in the northern flank of the Eastern Interior Range. No major tributary is directly flooding into the gulf. On the southern coast, only few small and short gullies carry temporary minor terrigenous sediments within the gulf. To the north, the coast is arid and its sedimentary contribution in the gulf is almost negligible. To the west, the Manzanares River has a wide, elevated, humid catchment area within the Eastern Interior Range, but it does not directly flow into the gulf. An artificial channel has been dug in the 1970s to mitigate the Rio Manzanares floods (Grases, 1979, 1990), but this channel does not flow into the gulf (Fig. 2). The geological substratum of the gulf's watershed (S1) shows a contrast between two groups of lithologies: mica-schists, quartzites, and greenschist to the north, and claystones, siltstones, and sandstones to the south. The gulf substratum is thus dominated by siliciclastic rocks. Plio-Pleistocene limestones, calcareous sandstones and marls exist locally at the northern entrance of the gulf where they provide an additional minor carbonate contribution (Macsotay and Moore, 1974).

1.2. Bathymetry of the gulf and of its western entrance

The floor morphology of the Gulf of Cariaco shows four singularities (Fig. 2) (Caraballo, 1982a, b; Maloney, 1966; Morelock and Maloney, 1972; Morelock et al., 1972):

- the Guaracayal basin (GD in Fig. 2), an elongated pull-apart ~90 m deep along the EPF, in the south of the gulf (Audemard et al., 2007);
- the large Cerro Abajo Basin (CAB), ~ 70 m deep, which occupies most of the gulf;
- to the northwest, the Salazar Sill (SS), a 5 km-wide, 40- to 50 m-deep, irregular channel, which links the Cerro Abajo Basin to the western entrance of the gulf;
- at the western tip of the gulf, the Manzanares submarine canyon, ~3 km northwest of the Rio Manzanares delta and the city of Cumaná. This canyon accounts for a 1350-m depth difference between the western mouth of the gulf and the deepest part of the Cariaco Basin. The eastern flank of the canyon, which bounds the Rio Manzanares delta, is very steep (up to 20°C).

1.3. Upwelling on the eastern slope of the Cariaco Basin and anoxia in the Gulf of Cariaco

Prior works have suggested a strong anoxia in the Cariaco Basin and in the Gulf of Cariaco (Bonilla and Hui-Lin, 1979; Caraballo, 1982a; Miró Orell, 1974). In the basin, the anoxia established after the Last Glacial Maximum, due to an increase in the surface productivity (Lyons et al., 2003). Hydrological and geochemical investigations also evidenced present massive water exchanges and seasonal strong anoxia in the deepest part of the Gulf of Cariaco (Gade, 1961; Okuda, 1981, 1982; Okuda et al., 1974, 1978; Richards, 1960). It is suggested that these exchanges and anoxia result from a cyclic pattern of trade winds and a thermal stratification of isohaline waters (Fig. 3). The seasonal regime along the northern Venezuelan coast is controlled by the migration of the Inter-Tropical Convergence Zone (ITCZ) (Haug et al., 2001). Two different regimes are evidenced along the eastern slope of the Cariaco Basin and inside the gulf (Fig. 3): a strong upwelling period (A) from February to June, during which flows of cold water are moving upward, and a weak upwelling period (B) between July and December. Upwelled cold and dense subsurface waters flow from the Cariaco Basin into the gulf; they bypass the 50 m-deep Salazar sill, and then move along the bottom of the gulf (for density reasons) towards its innermost parts (Caraballo, 1982a). This cold flow merges with the overall gulf water when it reaches the eastern part of the gulf. During these phases of cold-water renewal in the gulf, the oxygen content is increased. By contrast, during the periods of moderate to null renewal of cold bottom water in the gulf, the oxygen content decreases by 0.2–0.5 ml/l (Okuda, 1982).

Bonilla and Hui-Lin (1979) have suggested that the high concentration in organic matter found in the sediments of the gulf may result from both a high primary productivity and the upwelling process. Interflows rich in organic suspended loads have actually been observed to enter the

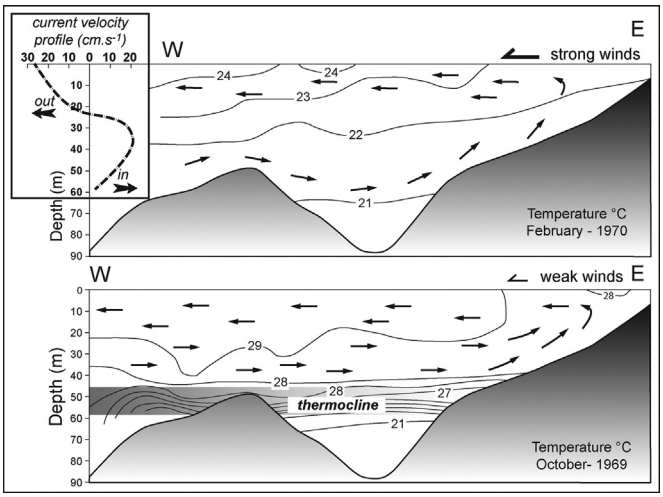

Fig. 3. Seasonal thermal situation and hydrodynamic connections between the Gulf of Cariaco and the Cariaco Trough. Compilation from Caraballo (1982a and b), Okuda (1981, 1982), and Gade (1961).

gulf (Okuda et al., 1974, 1978). Upwelling processes thus significantly affect the sedimentary content in the Gulf of Cariaco. While these upwelling processes are mainly controlled by climatic changes, they might also occur following a significant change in the submarine morphology of the gulf entrance (especially the Manzanares canyon and the Salazar Sill). We will pay a particular attention to this later possibility in the following.

2. Core acquisition and analyses

We extracted and analyzed sedimentary cores in the Gulf of Cariaco to search for possible changes in the sedimentary content that might attest to morphological and topographic changes in the basin–gulf system. The sedimentary signature of morphological changes in small-sized basins (lacustrine or marine) has been revealed in prior works, based on core data (Avşar, 2013; Avşar et al., 2015; Beck, 2009; Beck et al., 2007; Campos et al., 2013; Carrillo et al., 2008). The cores were collected onboard the R/V GUAIQUERI II, operated by the Eastern Oceanographic Institute (Instituto Oceanográfico de Oriente, Universidad de Oriente, Cumaná). We used a gravity piston corer based on the classical BENTHOS design, with a 6-cm internal diameter. The cores have an average length of 1 m.

The coring sites (location in Fig. 2) were selected with two main targets: 1) to define the depositional processes and sediment sources in the Gulf of Cariaco, and 2) to identify the possible impacts of EPF fault large earthquakes on the sedimentation. Four cores are distributed along an east–west trend across the Guaracayál depression. Four other cores were extracted 5 km to the north, in the Cerro Abajo depression. A third set of cores was extracted so as to complete a north–south line that would intersect the east–west section. In the following, we present only the results from the cores Cariac-09-05, Cariac-09-06, Cariac-09-15 and Cariac 09-18 (Fig. 2). Fig. 4 shows their position along a north–south 3.5 kHz seismic reflection profile (Van Daele et al., 2011).

Laboratory analyses encompass different nondestructive measurements and imaging, and different geochemical, mineralogical, and microscopic observations. The procedures are described in Supplementary Material S2.

3. Result analysis: recent sedimentation in the central and southern Gulf of Cariaco

3.1. Sediment layering and composition

In all analyzed cores, the sediments appeared homogenous and organic, made of a continuous fine-grained mud (hemipelagic fraction). High-resolution X-ray pictures (SCOPIX) did not reveal any layering, with the exception of a few coarse terrigenous layers (left log in Fig. 5). Rare macrofossils (thin-shelled bivalves, 1 to 2 cm in size, Turitella-type Gastropods, and few Dentalium-type Pteropods) were found dispersed within the organic-rich mud. Microscopic observations of the hemipelagic mud (smear slides and SYSMEX pictures) revealed clayey aggregates with clay-sized opaque and micritic particles. A siliceous biogenic material was found in significant proportion, mostly in the form of Diatoms and Silicoflagellids. Silt-size fibrous O.M. was found to be only a minor component.

3.2. General chemical evolution: XRD elementary profiles

Since the sedimentary features and chemical characteristics are clear in core Cariac-09-06, we take it as a reference. Fig. 5 shows the XRF profiles of the elements that we consider as best attesting to the presence of terrigenous siliciclastic inputs (Zr, Fe) or carbonates (Ca), or for open marine influence (Br). The similarity of the Al, Si, and K profiles confirms that these three elements describe the evolution of the clay mineral content adequately. Three siliciclastic layers (noted $SiCL_i$) are identified in the K, Zr and Fe profiles, where each forms a clear peak (i.e. increase of concentration). Pronounced variations coincident with the three peaks are observed in

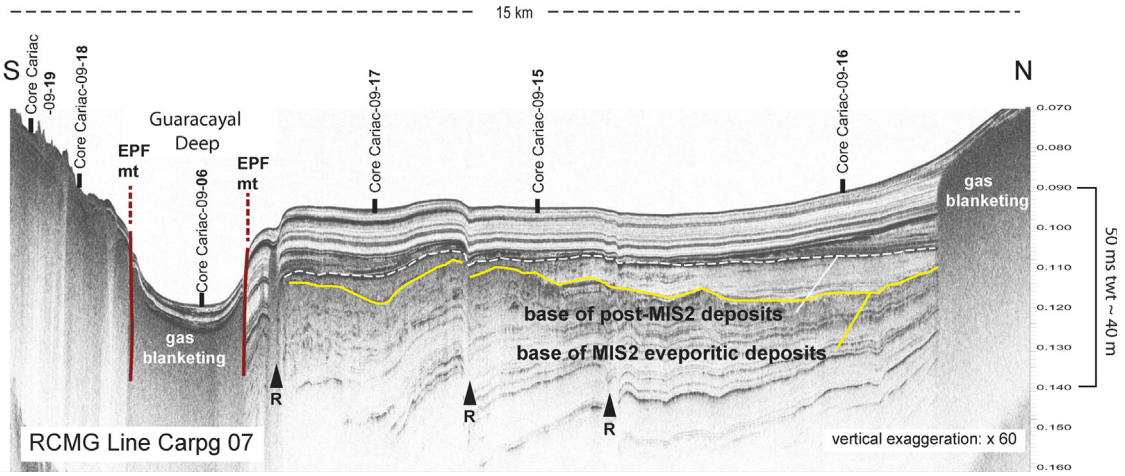

Fig. 4. (Color online). Location of cores along a very-high-resolution seismic section across the central Gulf of Cariaco (profile location in Fig. 2); EPFmt: El Pilar Fault main active trace (Audemard et al., 2007); R: minor faults (Van Daele et al., 2011).

the Al, Si, K (increased content) and $CaCO_3$ (decreased content) profiles. Two of the siliciclastic layers are characterized by coarse grains (Section 3.5). By contrast, the SiCL3 layer is only distinguishable on the XRF profiles where it forms a peak similar to those formed by SiCL1 and SiCL2 (Fig. 5). The three layers are also characterized by a decrease in O.M. content (Section 3.3). Furthermore, the bromine (Br) content systematically decreases in the three SiCL layers. However, subsequently to a Br decrease in layer SiCL3 in core Cariac-09-06 (Guaracayal deep), the Br content increases progressively in cores Cariac-09-15 (central gulf) and Cariac-09-18 (close to southern coast).

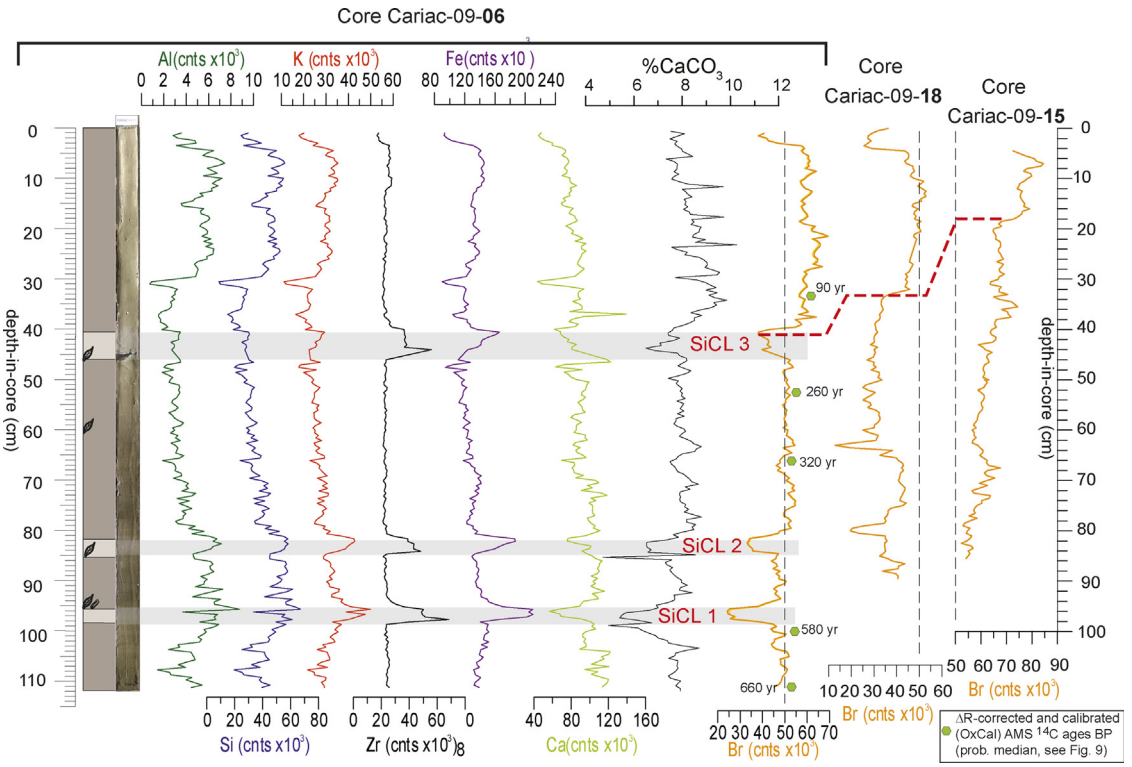

Fig. 5. (Color online). XRF scanning data from core Cariac-09-06. $SiCL_i$: siliciclastic layers; Br profiles for cores Cariac-09-18 (close to southern coast) and Cariac-09-15 (Gulf center) are shown to discuss correlations and signification of post-SiCL3 increase in Br; dotted vertical line as a reference value for comparison (note that Cariac-09-18 displays a similar Br evolution, but for lower values). BP ages correspond to probabilistic median of calibrated values distribution; the 2σ interval is indicated in Fig. 9.

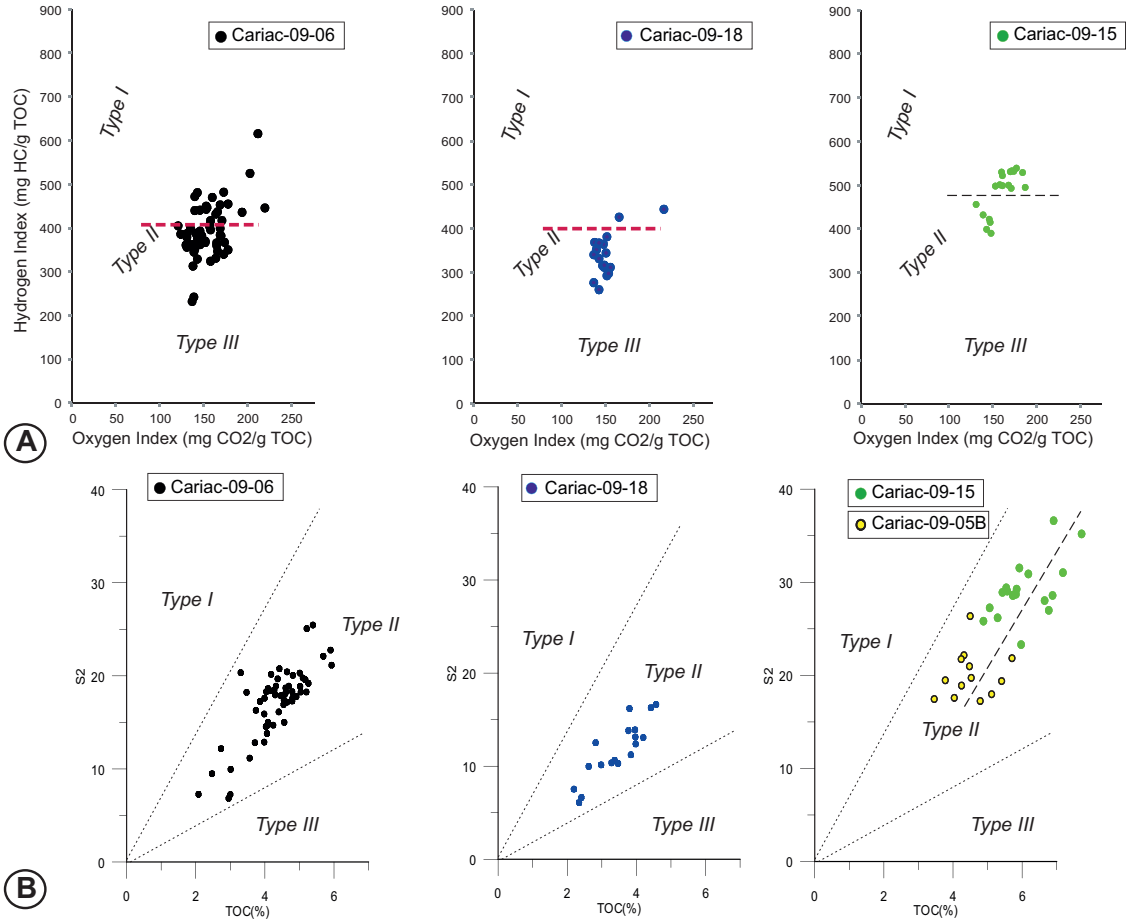

Fig. 6. (Color online). Characterization of O.M. by Rock-Eval pyrolysis. Graphs labeled A) modified Van Krevelen diagram, graphs labeled B) S2 peak vs. TOC diagram (Langford and Blanc-Valleron, 1990). The diagrams evidence a dominant type-II (marine) O.M. content for cores Cariac-08-06, Cariac-08-18 (close to southern coast), and Cariac-08-15 (Gulf center); core Cariac-08-06 is enriched in type-III (continental) O.M., while core Cariac-08-15 contains purely marine O.M., and core Cariac-08-06 includes a combination of the two groups of O.M. origin (separation by an horizontal red dashed line). In cores Cariac-08-18 (green dots) and Cariac-08-05 (yellow dots), the type-II O.M. samples may be divided into two sub-groups (separation by a black dashed line).

3.3. Organic matter content and characteristics

Rock-Eval pyrolysis results on the three cores along the north–south profile (Fig. 4) are summarized in Fig. 6 with respect to Total Organic Carbon (TOC), S2 peak, Hydrogen Index (HI), and Oxygen Index (OI). Diagrams labeled A represent the OI/HI plots similar to the Van Krevelen diagrams (Espitalié et al., 1985; Lafargue et al., 1998). Diagrams labeled B represent TOC *vs.* S2 HC as proposed by Langford and Valleron (1990). At all sites, O.M. appears of dominantly marine origin (type II), and is hardly or not altered. In core Cariac-09-18, close to the southern coast, the samples are dominated by type III, which suggests a terrestrial origin for O.M. In core Cariac-09-06, two major groups can be discriminated (separated by the red dashed line in Fig. 6): part of the samples have their O.M. attesting to a purely marine origin, whereas the other part of the samples have their O.M. attesting to a mixed marine and terrestrial nature. In core Cariac-09-15, the diagrams reveal that O.M. is of purely marine origin. Two subsets can be discriminated however (dashed line in Fig. 6). Similar subsets are found in core Cariac-09-05B and their values have been added onto diagram B (yellow dots) for comparison. We interpret the two subsets as revealing an O.M. content of two different origins: i) *in situ* production, and ii) input from the eastern Cariaco Basin likely from upwelling.

3.4. Occurrence of coarser and/or more siliciclastic layers (SiCL)

The observation of several split cores reveals the occurrence of two coarser siliciclastic layers, which we named SiCL1 and SiCL2 in Figs. 5 and 7. On X-ray pictures, another siliciclastic layer is revealed (SiCL3), which appears different from SiCL1 and SiCL2. We showed earlier that the three layers are terrigenous, and more precisely siliciclastic (Section 3.3). Grain-size analysis of cores Cariac-09-18, Cariac-09-15, Cariac-09-06, and Cariac-09-05B shows that a sandy fraction is present only close to the southern coast. The XRF profile of core Cariac-09-18 (Fig. 7) reveals two clear peaks coincident with an increase

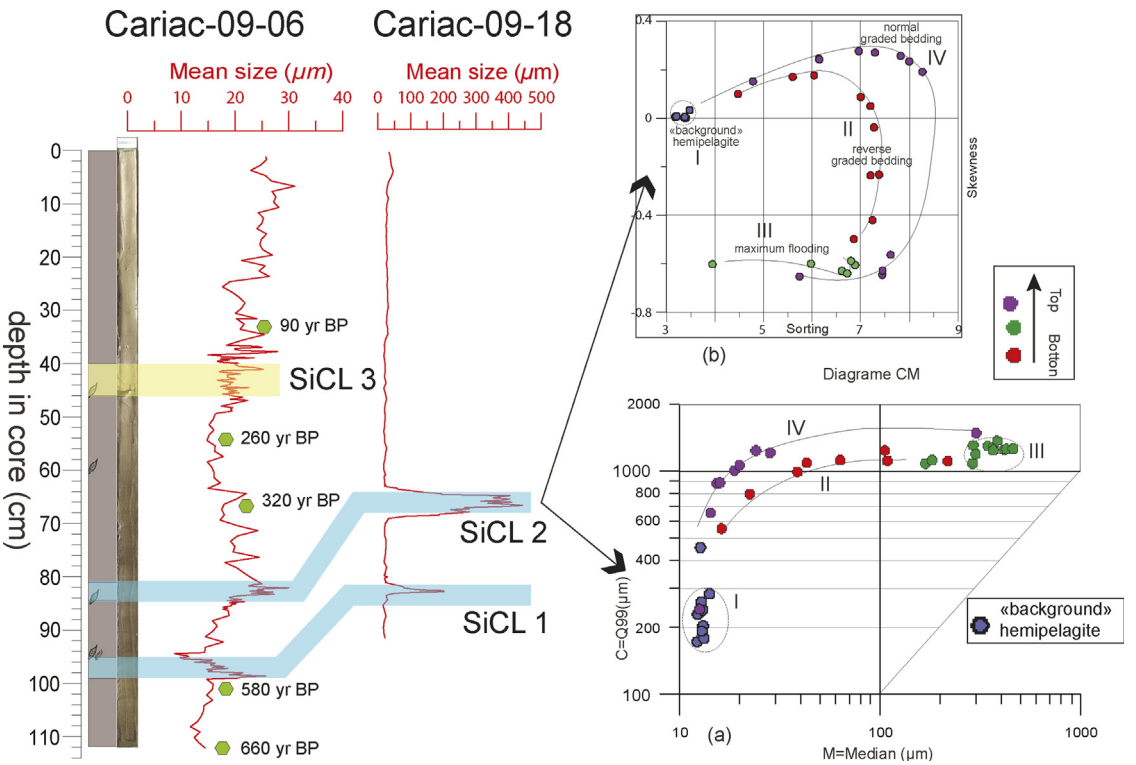

Fig. 7. (Color online). Grain-size evolution in cores Cariac-09-06 and Cariac-08-18 and characterization of the siliciclastic layers. The base-to-top paths for SiCl-1 and SiCl-2 indicate flooding events (Beck, 2009); SiCl-3 does not show any coarser fraction; its terrigenous (siliciclastic) content enrichment is only indicated by chemical parameters (XRF, Fig. 6). BP ages are reported as in Fig. 5.

in silt-size grains in core Cariac-09-06. The siliciclastic enrichment in the other cores–including those in the gulf center–is clayey or clayey–silty, i.e. related to suspended-load transport and deposition.

The base-to-top evolution of both the SiCL1 and SiCL2 layers (Fig. 7) is typical of sediment evolutions related to flooding processes (Beck, 2009). Therefore, SiCL1 and SiCL2 do not result from gravity reworking processes. Rather, these layers likely arise from inputs from southern tributaries. In contrast, the SiCL3 layer appears as a widespread input of fine-grained siliciclastic material. We suggest that this widespread (suspended-load) input is an allochthonous terrigenous feeding coming from the western entrance of the gulf, likely induced by upwelling.

3.5. Chronology and mean sedimentation rate

The different investigated parameters confirm the importance of suspended-load coming from the Cariaco Basin, including "allochthonous" O.M. attesting to a more open marine influence. The regional ΔR was found due to the above-mentioned process. Therefore, this type of correction was applied to the age–depth curve of cores Cariac-09-06 and Cariac-09-5B (Supplementary Material S3). In both cores, a mean sedimentation rate of 1.0 to 1.2 mm/yr was deduced. If the SiCL layers are taken as sedimentary "events", then the "normal sedimentation" rate might be slightly lower. Considering the correlations that we proposed between cores Cariac-09-06 and Cariac-09-15 for the SiCL3 layer (S3), we infer that the sedimentation rate might be lower in the central gulf.

4. Discussion

The recent dominant sedimentation in the central and southern parts of the Gulf of Cariaco, along and adjacent to the EPF fault trace, is organic-rich, finely terrigenous, and poorly layered. Biogenic and bio-induced components are essentially planktonic. The high particulate organic content (up to 5% TOC or 20% O.M., Fig. 8A) appears of dominant marine origin (type II), yet with two different possible sources: local production, and a general input from the eastern Cariaco Basin likely by mean of upwelling. The bromine content displays an evolution consistent with a significant open marine influence (Thomson et al., 2006; Ziegler et al., 2008). According to the ^{14}C dating and the chronology we have inferred (S3), the open marine influence might have started around 1850 AD. We are aware that the Br evolution must be discussed with respect to the O.M. content, since their combined short-term diagenesis may induce Br changes. Yet, the evolution of Br and O.M. is different below and above the layer SiCL3 (Br *vs.* O.M. and Br *vs.* TOC, Fig. 8B and Fig. 8C), which suggests that they are not directly linked. We thus interpret the post-SiCL3 increase in Br evolution as attesting to a more marine influence related to an increase in upwelling-driven input (water and suspended load) from the Cariaco Basin.

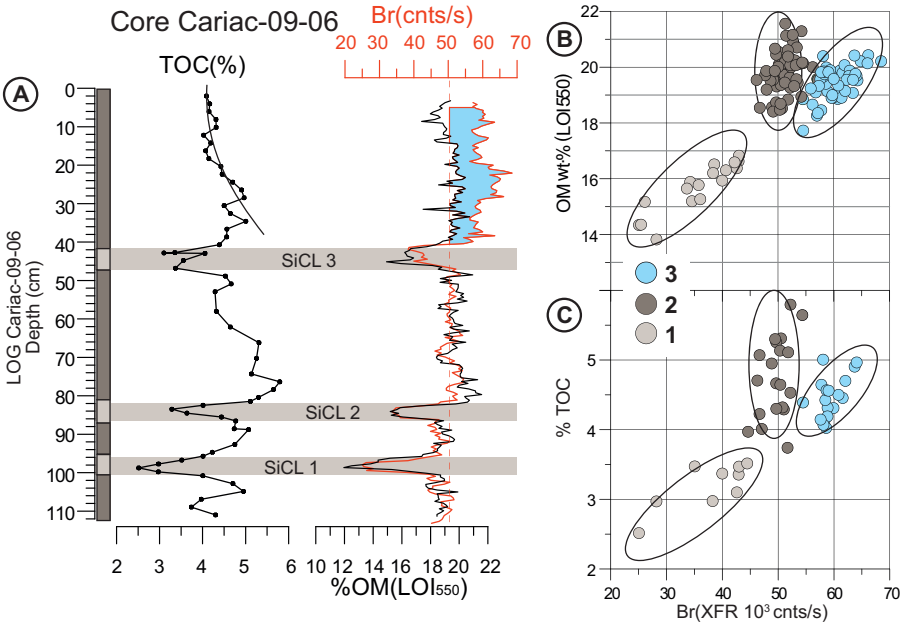

Fig. 8. (Color online). Comparison of Br and O.M. profiles in Core Cariac-09-06. The O.M. content is represented by LOI measurements and COT deduced from Rock-Eval pyrolysis. The post-SiCL3 Br increase is disconnected form the O.M. evolution (A); O.M. vs. Br diagrams (B and C) confirm this discrimination for the upper 40 cm of hemipelagic sediments; 1) samples within siliciclastic layers, 2) samples in organic mud prior to SiCL3, 3) samples in organic mud after SiCL3.

Such an upwelling increase could have resulted from: i) a reinforcement of the winds, ii) a modification of the gulf's entrance geometry. Paleoclimatic investigations in northwestern Venezuela (Polissar et al., 2006) indicate strong easterly trade winds during the Little Ice Age, which ended in the middle of the 19th century. These findings do not support the reinforcement of trade winds in the second half of the 19th century. Conversely, the geometrical modification (bottom morphology, depth) of the basin–gulf connection is a reasonable hypothesis knowing the great instability of the area. We thus consider that the open marine signature reveals significant water flows from the Cariaco Basin, induced by upwelling resulting from a major morphological change at the basin–gulf junction.

The southern half of the gulf's entrance corresponds to the steep western boundary of the Rio Manzanares delta (Fig. 2). High-resolution seismic profiles shot in the delta reveal the occurrence of large recent landslides (called Mass Transport Deposits or MTDs in Fig. 9) that accumulated at the foot of the delta. Their large volumes and their addition over time may have significantly modified the morphology and topography of the connection between the gulf and the basin. It is likely that some or even most of these landslides were induced by large earthquakes on the EPF fault, as it was observed right after the 1997 earthquake (the harbor of Cumaná underwent local piers collapses during the earthquake).

We thus interpret the SiCL3 layer as a sedimentary "event" related to one or to several Mass Transport Deposits on the western side of the Manzanares River delta. The layer could represent a fine-grained suspension as the one observed after the 1997 earthquake. The layer would thus indirectly testify for a large earthquake. During the 1853 AD event, a 4- to 6 m-high tsunami wave was reported. The time of formation of SiCL3 is consistent with the earthquake time. Therefore, we suggest that the SiCL3

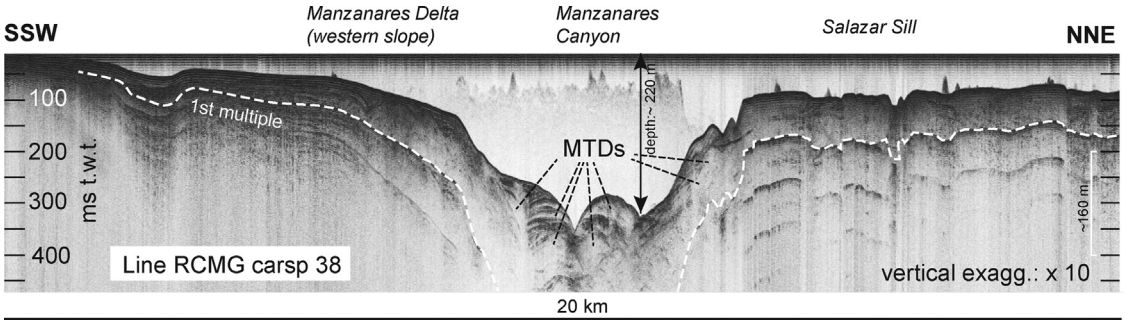

Fig. 9. High-resolution seismic profile across Gulf of Cariaco's entrance, displaying the accumulation of MTDs (profile location in Fig. 2).

layer was formed as a result of one or several large, coeval submarine landslides that were induced by intense shaking during the 1853 earthquake. The submarine landslides significantly modified the topography of the gulf's entrance, and these modifications promoted significant water flows from the open marine Cariaco Basin.

Conclusions

Our results confirm that the sedimentation in the central and the southern Gulf of Cariaco is significantly fed by upwelling at the western entrance of the gulf. We found evidence for a well-expressed, widespread, siliciclastic event (SiCL3), which we interpret as being the fine-grained material remobilized during an important submarine land sliding along the Manzanare River delta foreset. This major land sliding episode would have significantly modified the topography of the connection between the Cariaco Basin and the Gulf of Cariaco, and these changes would have promoted upwelling and entrance of open marine water flows into the gulf. We suggest that land sliding was induced by the large 1853 AD earthquake that struck the Cumaná city. Further work is needed to validate these hypotheses, which concerns the appraisal of earthquake-related risks for the city and its harbor. Finally, the present investigations show that earthquake record in sedimentary archives may be detected through varied parameters, each case needing however specific approaches.

Acknowledgements

This paper has been written in tribute to Jean-François Stéphan, who initiated, thirty years ago, a fruitful and still developing Venezuelan-French cooperation in earth sciences; two of us (CB and FA) had the great privilege of sharing his friendship and his permanent enthusiasm during field research. The investigations were realized thanks to a Venezuelan-French ECOS-Norte grant No. V10U01. I. Aguilar's stay in ISTerre Laboratory and PhD preparation were achieved thanks to a PhD grant funded by Fundayacucho (Venezuelan PhD Grants Program). We also acknowledge Funvisis (Venezuela Foundation for Seismological Investigations) and CNRS ISTerre (Earth Sciences Institute, Grenoble Alps University) for additional funding of laboratory analyses. Coring campaign was performed thanks to the whole crew of R/V Guaiqueri II and Andres Lemus, head of Camudoca. We acknowledge Rachel Boscardin at ISTO Orléans for guiding Rock–Eval analyses. This paper has been reviewed by Klaus Reicherter and Aurélia Hubert-Ferrari, and by Associate Editor Isabelle Manighetti; many thanks for their contribution to the improvement of our initial manuscript.

Appendix A. Supplementary data

Supplementary data associated with this article can be found, in the online version, at http://dx.doi.org/10.1016/j.crte.2015.10.001.

References

Altez Ortega, R., Rodriguez, J.A., Urbani, F., 2004. Historia del pensamiento sismológico en Venezuela. Ed. UCV-FUNVISIS, Caracas.

Audemard, F.A., 2007. Revised seismic history of the El Pilar fault, northeastern Venezuela, from the Cariaco 1997 earthquake and recent preliminary paleoseismic results. J. Seismology 11 (3), 311–326.

Audemard, F.A., Beck, C., Moernaut, J., De Rycker, K., De Batist, M., Sánchez, J., González, M., Sánchez, C., Versteeg, W., Malavé, G., Schmitz, M., Van Welden, A., Carrillo, E., Lemus, A., 2007. La depresión de Guaracayál. estado Sucre. Venezuela: una cuenca en tracción que funciona como barrera para la propagación de la ruptura cosísmica. Interciencia 32 (11), 735–741.

Audemard, F.A., Machette, M.N., Cox, J.W., Dart, R.L., Haller, K.M., 2000. Map of Quaternary faults of Venezuela. USGS Open-File report 00-0018.

Audemard, F.A., Romero, G., Rendon, H., Cano, V., 2005. Quaternary fault kinematics and stress tensors along the southern Caribbean from fault-slip data and focal mechanism solutions. Earth-Sci. Rev. 69 (3–4), 181–233, http://dx.doi.org/10.1016/j.earscirev.2004.08.001.

Avşar, U., 2013. Lacustrine paleoseismic records from the North Anatolian Fault, Turkey. PhD, University of Gent, 209 p.

Avşar, U., Hubert-Ferrari, A., De Batist, M., Schmidt, S., Fagel, N., 2015. Sedimentary records of past earthquakes in Boraboy Lake during the last ca 600 years (North Anatolian Fault, Turkey). Palaeogeogr. Palaeoclimatol. Palaeoecol. 43, 1–9.

Beck, C., 2009. Late Quaternary lacustrine paleo-seismic archives in north-western Alps: Examples of earthquake-origin assessment of sedimentary disturbances. Earth-Sci. Rev. 96, 327–344.

Beck, C., Mercier de Lépinay, B., Schneider, J.-L., Cremer, M., Çağatay, N., Wendenbaum, E., Boutareaud, S., Ménot, G., Schmidt, S., Weber, O., Eris, K., Armijo, R., Meyer, B., Pondard, N., Gutscher, M.-A., and the MARMACORE Cruise Party, Turon, J.-L., Labeyrie, L., Cortijo, E., Gallet, Y., Bouquerel, H., Gorur, N., Gervais, A., Castera, M.-H., Londeix, L., de Rességuier, A., Jaouen, A., 2007. Late Quaternary co-seismic sedimentation in the Sea of Marmara's deep basins. Sediment. Geol. 19, 65–89.

Bonilla, J., Hui-Lin, H.L., 1979. Materia orgánica en los sedimentos de los Golfos de Paria y Cariaco. Boletín del Instituto Oceanográfico de Venezuela 18, 37–52.

Campos, C., Beck, C., Crouzet, C., Demory, F., Van Welden, A., Eris, K., 2013. Deciphering hemipelagites from homogenites through anisotropy of magnetic susceptibility. Paleoseismic implications (Sea of Marmara and Gulf of Corinth). Sediment. Geol. 292, 1–14.

Caraballo, L.F., 1982a. El Golfo de Cariaco. II: Los sedimentos superficiales, y su distribución por el fondo. Fuente de sedimentos. Análisis mineralógico. Boletín del Instituto Oceanográfico de la Universidad de Oriente 21 (1–2), 37–65.

Caraballo, L.F., 1982b. El Golfo de Cariaco. III: Contenido de carbonatos y constituyentes de las partículas de los sedimentos. Su distribución por el fondo. Fauna característica. Boletín del Instituto Oceanográfico de la Universidad de Oriente 21 (1–2), 67–83.

Carrillo, E., Beck, C., Audemard, F.A., Moreno, E., Ollarves, R., 2008. Disentangling Late Quaternary climatic and seismo-tectonic controls on Lake Mucubají sedimentation (Mérida Andes, Venezuela). Palaeogeogr. Palaeoclimatol. Palaeoecol. 259, 284–300.

DeMets, C., Jansma, P.E., Mattioli, G.S., Dixon, T.H., Farina, F., Bilham, R., Calais, E., Mann, P., 2000. GPS geodetic constraints on Caribbean-North America plate motion. Geophys. Res. Lett. 27 (3), 437–440.

Espitalié, J., Deroo, G., Marquis, F., 1985. La pyrolyse Rock-Eval et ses applications Deuxième partie. Oil Gas Sci. Technol. 4, 755–784.

Gade, H.G., 1961. Further hydrographic observation in the Gulf of Cariaco, Venezuela. The circulation and water exchange. Boletín del Instituto Oceanográfico de la Universidad de Oriente 1 (2), 359–395.

Garrity, C., Hackley, P., Urbani, F., 2004. Digital shaded-relief map of Venezuela. , http://pubs.usgs.gov/of/2004/1322.

Grases, J., 1979. Investigaciones sobre los sismos destructores que han afectado el oriente de Venezuela, Delta del Orinoco y regiones adyacentes. INTEVEP Report, 107 p.

Grases, J., 1990. Terremotos destructores del Caribe. 1502–1990. 1º ed. Unesco-Relacis.

Haug, G.H., Hughen, K.A., Sigman, D.M., Peterson, L.C., Rölh, U., 2001. Southward migration of the intertropical convergent zone through the Holocene. Science 293 (5533), 1304–1308.

Jouanne, F., Audemard, F.A., Beck, C., Van Welden, A., Ollarves, R., Reinoza, C., 2011. Present-day deformation along the El Pilar Fault in eastern Venezuela. Evidence of creep along a major transform boundary. J. Geodyn. 51, 398–410.

Lafargue, E., Marquis, F., Pillot, D., 1998. Rock-Eval 6 applications in hydrocarbon exploration, production, and soil contamination studies. Oil Gas Sci. Technol. 53, 421–437.

Langford, F.F., Blanc-Valleron, M.-M., 1990. Interpreting Rock-Eval Pyrolysis Data Using Graphs of Pyrolizable Hydrocarbons vs Total Organic Carbon (1). AAPG Bull. 74, 799–804.

Leal, K., Scremin, L., Audemard, F., Carrillo, E., 2014. Paleotsunamis en el registro geológico de Cumaná, Estado Sucre, Venezuela oriental. Boletín de Geología 36 (2), 45–70.

Lorenzoni, L., Benitez-Nelson, C.R., Thunel, R.C., David Hollander, D., Varela, R., Astor, Y., Audemard, F.A., Muller-Karger, F.E., 2012. Potential role of event-driven sediment transport on sediment accumulation in the Cariaco Basin, Venezuela. Mar. Geol. 307, 105–110.

Lyons, T.W., Werne, J.P., Hollander, D.J., Murray, R., 2003. Contrasting sulfur geochemistry and Fe/Al and Mo/Al ratios across the last oxic-to-anoxic transition in the Cariaco Basin, Venezuela. Chem. Geol. 195 (1), 131–157.

Macsotay, O., Moore, W.S., 1974.In: Cronoestratigrafía de algunas terrazas cuaternarias marinas del Nororiente de Venezuela. *Cuadernos Azules*, III Conferencia de las Naciones Unidas sobre el Derecho del Mar, vol. 12, pp. 1–63.

Maloney, N., 1966. Geomorphology of continental margin of Venezuela, Part I, Cariaco Basin. Boletín del Instituto Oceanográfico de la Universidad de Oriente 5, 38–53.

Miró Orell (de), M., 1974.In: Cuadernos Azules, III Conferencia de las Naciones Unidas sobre el Derecho del Mar, vol. 14, pp. 1–230.

Morelock, J., Maloney, N., 1972. Manzanares Submarine Canyon. Acta Científica Venezolana 23, 143–147.

Morelock, J., Maloney, N., Bryant, W., 1972. Structure and sediments of the continental shelf of central Venezuela. Boletín del Instituto Oceanográfico de la Universidad de Oriente 11, 127–136.

Okuda, T., 1981.In: Water exchange and the balance of phosphate in the Gulf of Cariaco Venezuela, Coastal Upwelling, pp. 274–281.

Okuda, T., 1982. Rate of water renewal and phosphate input in the Cariaco Gulf, Venezuela. Boletín del Instituto Oceanográfico de la Universidad de Oriente 21 (1–2), 3–12.

Okuda, T., Bonilla Ruiz, J., Garcia, A.J., 1974. Algunas caracteristicas bioquimicas en el agua de la Fosa de Cariaco. Boletin del Instituto Oceanografico de la Universidad de Oriente 13, 163–174.

Okuda, T., Benitez-Alvarez, J., Bonilla, J., Cedeño, G., 1978. Características hidrográficas del golfo de Cariaco, Venezuela. Boletin del Instituto Oceanografico de la Universidad de Oriente 17, 69–88.

Pérez, O., Bilham, R., Bendick, R., Hernández, N., Hoyer, M., Velandia, J., Moncayo, C., Kozuch, M., 2001. Velocidad relativa entre las placas del Caribe y Sudamérica a partir de observaciones dentro del sistema de posicionamiento global (GPS) en el norte de Venezuela. Interciencia 6 (2), 69–74.

Polissar, P.J., Abbott, M.B., Wolfe, A.P., Bezada, M., Rull, V., Bradley, R.S., 2006. Solar modulation of Little Ice Age climate in the tropical Andes. Proc. Natl. Acad. Sci. U. S. A. 103 (24), 8937–8942.

Reinoza, C., Jouanne, F., Audemard, F.A., Schmitz, M., Beck, C., 2015. Geodetic exploration of strain along the El Pilar Fault in northeastern Venezuela. J. Geophys. Res. Solid Earth 1993–2013, http://dx.doi.org/10.1002/2014JB011483.

Richards, F.A., 1960. Some chemical and hydrographic observations along the north coast of South America—I. Cabo Tres Puntas to Curacao, including the Cariaco Trench and the Gulf of Cariaco. Deep Sea Res 7, 163–182.

Schubert, C., 1979. El Pilar Fault Zone, northeastern Venezuela: Brief review. Tectonophys. 5 (2), 447–455.

Schubert, C., 1982. Origin of Cariaco Basin, southern Caribbean Sea. Mar. Geol. 47, 345–360.

Stéphan, J.-F., Mercier de Lépinay, B., Calais, E., Tardy, M., Beck, C., Carfantan, J.-C., Olivet, J.-L., Vila, J.-M., Bouysse, P., Mauffret, A., Bourgois, J., Théry, J.-M., Tournon, J., Blanchet, R., Dercourt, J., 1990. Paleogeodynamic maps of the Caribbean: 14 steps from Lias to Present. Bull. Soc. geol. France 8 VI, 915–919 [14 appendices].

Symithe, S., Calais, E., de Chabalier, J.-B., Robertson, R., Higgins, M., 2015. Current Block Motions and Strain Accumulation on Active Faults in the Caribbean. J. Geophys. Res. Solid Earth 120, 3748–3774, http://dx.doi.org/10.1002/2014JB011779.

Thomson, J., Croudace, I., Rothwell, R., 2006. A geochemical application of the ITRAX scanner to a sediment core containing eastern Mediterranean sapropel units. Geol. Soc. London, Spec. Publ. 267 (1), 65–77.

Thunell, R., Tappa, E., Valera, R., Llano, M., Astor, Y., Muller-Karger, F., Bohrer, R., 1999. Increased marine sediment suspension and fluxes following an earthquake. Nature 398, 233–236.

Van Daele, M., van Welden, A., Moernaut, J., Beck, C., Audemard, F.A., Sanchez, J., Jouanne, F., Carrillo, E., Malavé, G., Lemus, A., De Batist, M., 2011. Reconstruction of Late-Quaternary sea- and lake-level changes in a tectonically active marginal basin using seismic stratigraphy: The Cariaco Gulf, NE Venezuela. Mar. Geol. 279 (1), 37–51.

Weber, J., Dixon, T., DeMets, C., Ambeh, W., Jansma, P., Mattioli, G., Saleh, J., Sella, G., Bilham, R., Pérez, O., 2001. GPS estimate of relative motion between the Caribbean and South American plates and geologic implications for Trinidad and Venezuela. Geology 29 (1), 75–78.

Ziegler, M., Jilbert, T., de Lange, G.J., Lourens, L.J., Reichart, G.J., 2008. Bromine counts from XRF scanning as an estimate of the marine organic carbon content of sediment cores. Geochem. Geophys. Geosys. 9 (5) , http://dx.doi.org/10.1029/2007GC001932.